POLITECNICO
MILANO 1863

Politecnico di Milano
Scuola di Ingegneria

MECHANICAL ENGINEERING: MECHATRONICS AND ROBOTICS

Academic Year 2025/2026

Advanced Dynamics of Mechanical Systems

Project Report

Authors:

Caterina Brunetti
Alessia Cecchini
Federico Della Vittoria
Tareq El Kajjyouy

June 2026

Dynamic Analysis of the CityWave Canopy

The analysis we'll perform is associated to a real structure: the *CityWave*, a canopy structure with a peculiar shape that will be part of the CityLife district buildings.

Our analysis is a comparison between modal and numerical result: we developed a *modal model* that then has been compared with the FEM solution provided by the professor.

The starting point is a dataset obtained from a wind-tunnel scaled model simulation: the excitation is a *swept sine* provided through a modal shaker and monitoring the response in 202 points through a laser doppler vibrometer.

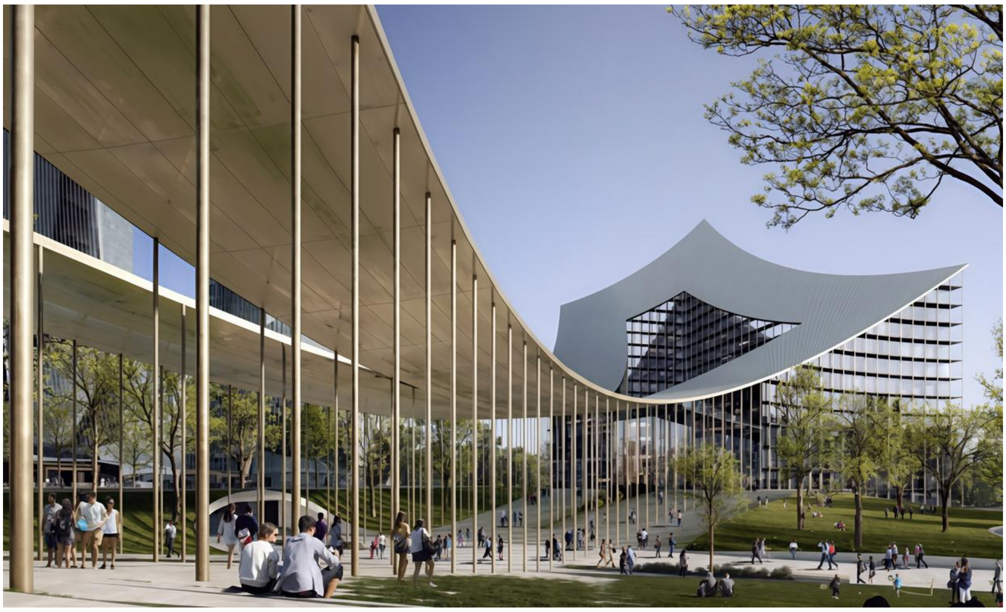

Figure 1.17: The Canopy of the CityWave in CityLife district.

1.2.7 Modal parameters identification

The presence of experimental data, which are characterized by a large amount of noise, and the FEM model of the system make quite interesting the analysis.

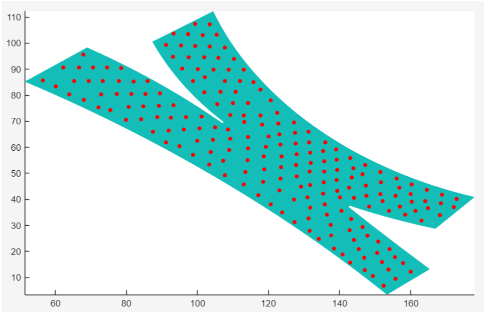

(a) 2D model and points of interest.

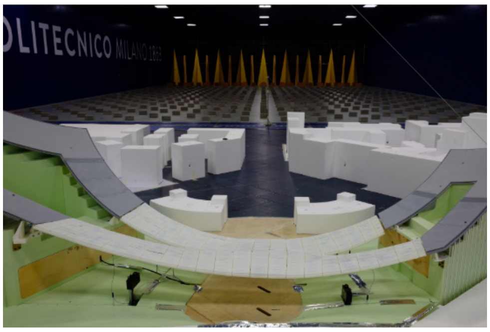

(b) The canopy model in the wind tunnel.

Figure 1.18: Modeling the structure.

The datasets used in this work are structured as follows:

`Connectivity`: it contains the geometric information regarding the nodes of the Finite Element Model (FEM) and their respective surface definitions.

`FRF_H1`: it includes all 202 Frequency Response Functions (FRFs) acquired/calculated for each sensor across a wide frequency range.

`punti_laser`: it provides the spatial coordinates (positions) of the laser sensors as well as the total sensor count.

`modal_output`: it contains the numerical mode shapes extracted from the FEM analysis.

`Students`: it consists of the plots and visual representations of the FEM mode shapes.

The frequency range on which we would like to represent the mode shapes of our interest is on the range $2 - 8\ Hz$.

Once the frequency range of interest has been defined and the data have been extracted, as we plot the magnitude and the phase of the FRFs with respect to all the sensors, we can notice the presence of noise and high complexity which makes the analysis more difficult. Indeed, we obtain the following:

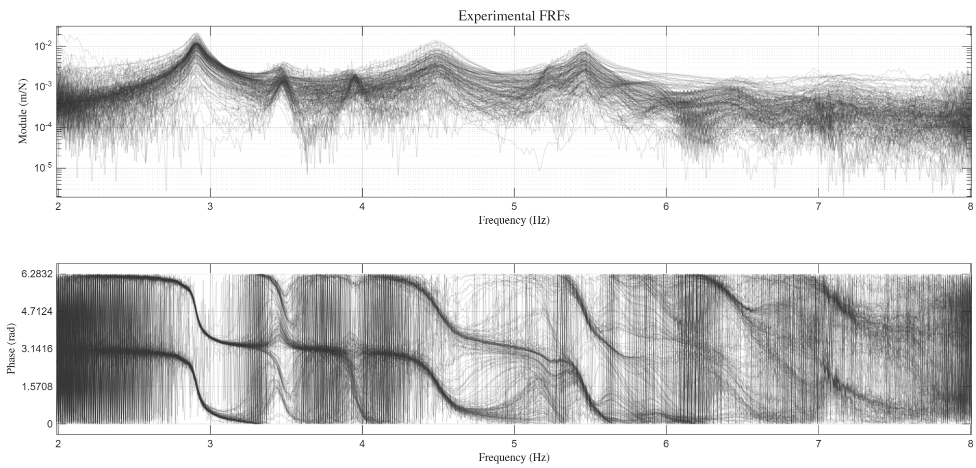

Figure 1.19: Module and phase diagrams of the experimental FRFs

Each curve represents the behavior of each FRF, and, as we have 202 sensors, we expect 202 FRFs.

To determine the eigenfrequencies, we rely on the application of the mean. The idea is to apply the average of the magnitudes on all the FRFs in order to obtain one unique curve for which we can rely on. Consequently, the index of the frequency associated to each peak of the curve is expected to be, *approximately*, the eigenfrequencies. As a result, the plot will be of this type:

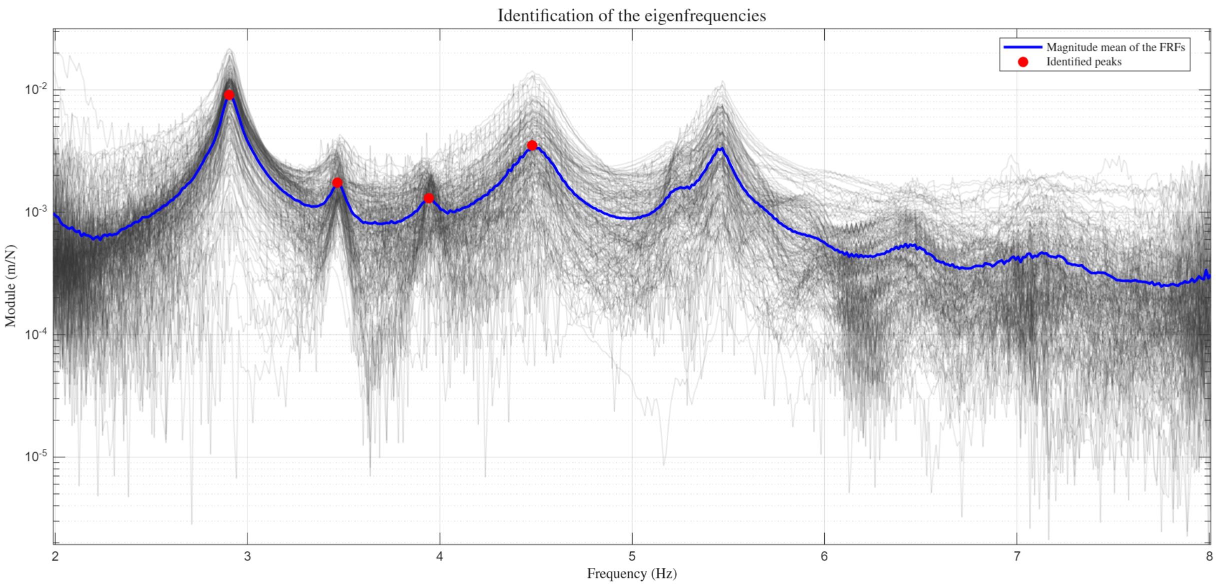

Figure 1.20: Identification of the eigenfrequencies based on the magnitude mean of the FRFs

Now that we have all the eigenfrequencies, as these tests are from an experiment conducted in the *wind tunnel*, it is necessary to scale the values we just obtained in order to make them compliant with the full scale. As a result, we are expected to obtain the following values:

Table 1.2: Comparison between wind tunnel and FEM natural frequencies

Mode	f_{WT} **before scaling (Hz)**	f_{WT} **after scaling (Hz)**	f_{FEM} **(Hz)**	**Error (%)**
1	2.905	0.347	0.339	2.43
2	3.466	0.414	0.454	8.73
3	3.942	0.471	0.498	5.36
4	4.479	0.535	0.572	6.38

The procedure carried out for the identification of the eigenfrequencies can be considered reliable because the error is very small.

The evaluation of the adimensional damping ratio has to be carried out for every mode and we relied on the *peak picking method*. To apply it, the Formula 1.14 has been exploited:

$$\xi_i = \frac{\omega_2^2 - \omega_1^2}{4\omega_i^2}\,, \tag{1.14}$$

where, for the i^{th} mode, ω_i corresponds to the natural frequency. ω_2 and ω_1 correspond to the angular frequencies associated to $\frac{\sqrt{2}}{2}|G(\omega_i)|$ and the relationship $\omega_2 > \omega_i > \omega_1$ is valid.

During the evaluation of the damping ratio of the i^{th} mode, we can't consider all the 202 FRFs, because the final result would be affected by both sensors in anti-nodal and nodal positions and by the possible presence of faulty sensors. A strategy needs to be set up in order to overcome this problem.

For every identified natural frequency, the algorithm evaluates the magnitude of the FRFs associated with all the available sensors. The sensor exhibiting the maximum FRF amplitude at the considered resonance peak is identified as the most representative for that mode. Once the maximum FRF amplitude is determined, a threshold equal to 80% of the peak value is introduced. This threshold is used to identify the sensors that are significantly involved in each mode shape. More specifically, only the sensors whose FRF magnitude exceeds the selected threshold are retained for the damping estimation procedure.

In the Figure 1.21, the FRFs in anti-nodal positions are shown for each mode of vibration.

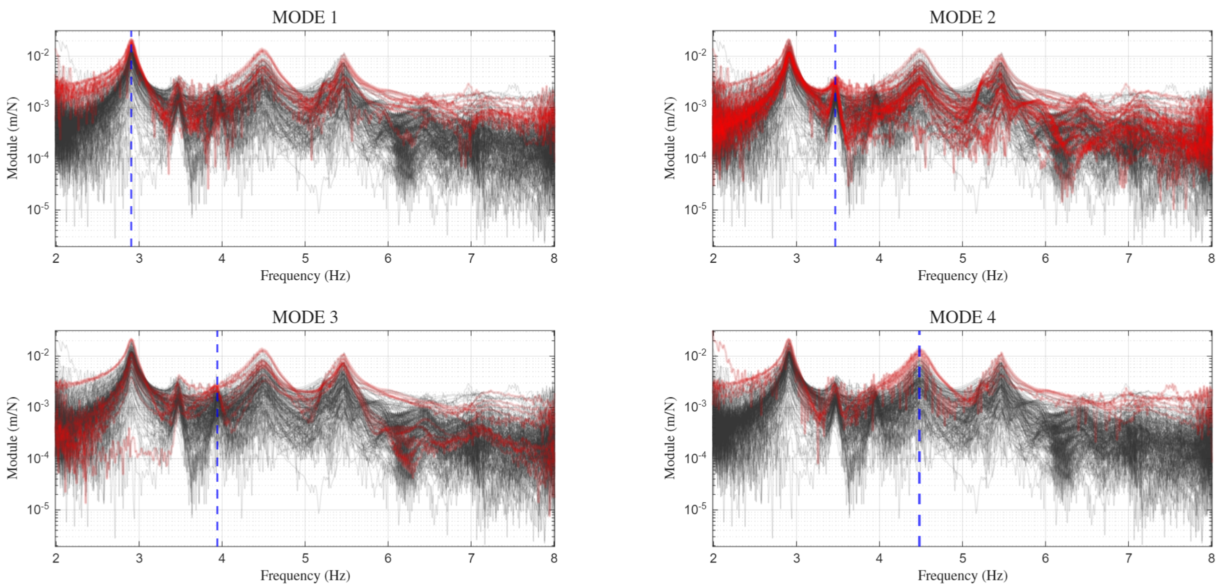

Figure 1.21: FRFs in anti-nodal positions

Then, for each mode, the mean of the selected FRFs has been performed and the corresponding graphs are shown in Figure 1.22.

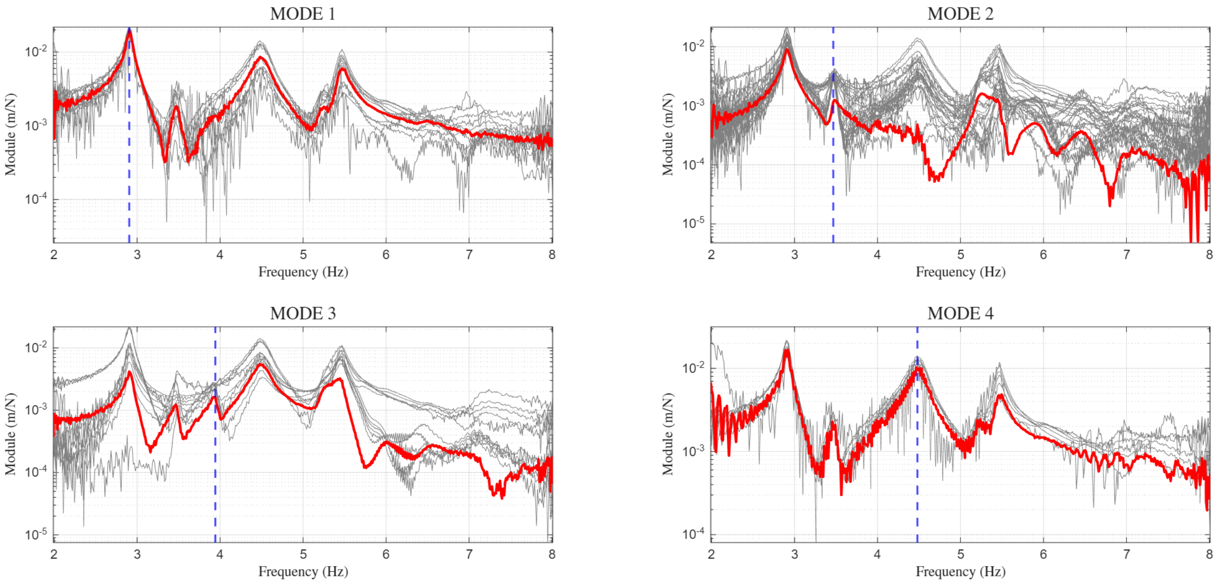

Figure 1.22: FRFs' mean

Consequently, an algorithm based on the equation 1.14 has been implemented in order to calculate the adimensional damping ratio for each mode. As a result, we obtained the damping ratios listed in Table 1.3.

Table 1.3: Adimensional damping ratios associated at each mode

Mode	f_{WT} **(Hz)**	ξ **(%)**
1	0.347	0.84
2	0.414	1.97
3	0.471	1.23
4	0.535	1.23

Finally, in order to conclude our modal parameter identification, we must determine the mode shapes values. To determine the mode shapes, we rely on the following formula:

$$\Phi_{ki}(x) = Imag(G_{ij}(\omega))\frac{\omega_k c_k}{\Phi_{kj}} \tag{1.15}$$

1.3 Plot of the FEM and EMA models

The **model validation** process is a critical step in structural dynamics, serving to verify that the numerical Finite Element (FE) model accurately reproduces the dynamic behavior of the actual physical system. This section describes the implementation of a side-by-side comparison between the natural frequencies and mode shapes obtained through numerical simulation (FEM) and those identified via *Experimental Modal Analysis* (EMA).

1.3.1 Spatial Representation of the Structure and Sensors

The overall geometry of the structure is established by mapping the nodes of the numerical model through their individual identification markers. To facilitate a clear evaluation of the experimental configuration, the physical points of measurement are projected directly onto the discrete numerical mesh. This procedure enables a visual confirmation of the spatial alignment between the system's numerical degrees of freedom and the actual physical locations where the dynamic response was recorded.

The comparison between EMA analysis and FEM analysis is not straight forward. Since the numerical mesh of the FEM has much more nodes than the 202 sensors' positions, once we calculated the mode shapes over all the sensors' points, we performed an interpolation over the nodes of the numerical mesh.

As a result, now it is possible to compare the FEM and EMA model. The visual comparison is shown in Figures 1.23, 1.24, 1.25 and 1.26.

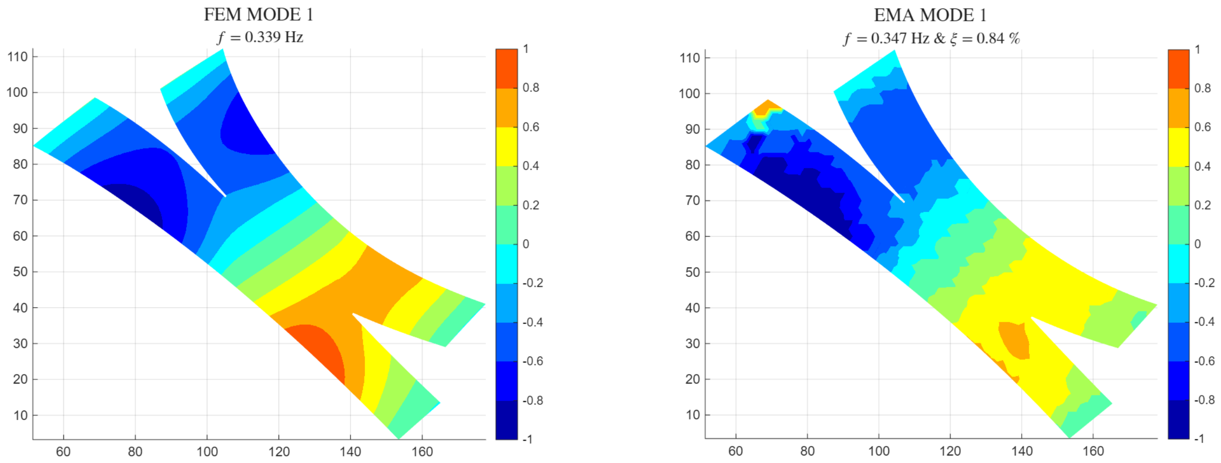

Figure 1.23: Comparison between FEM and EMA of mode 1

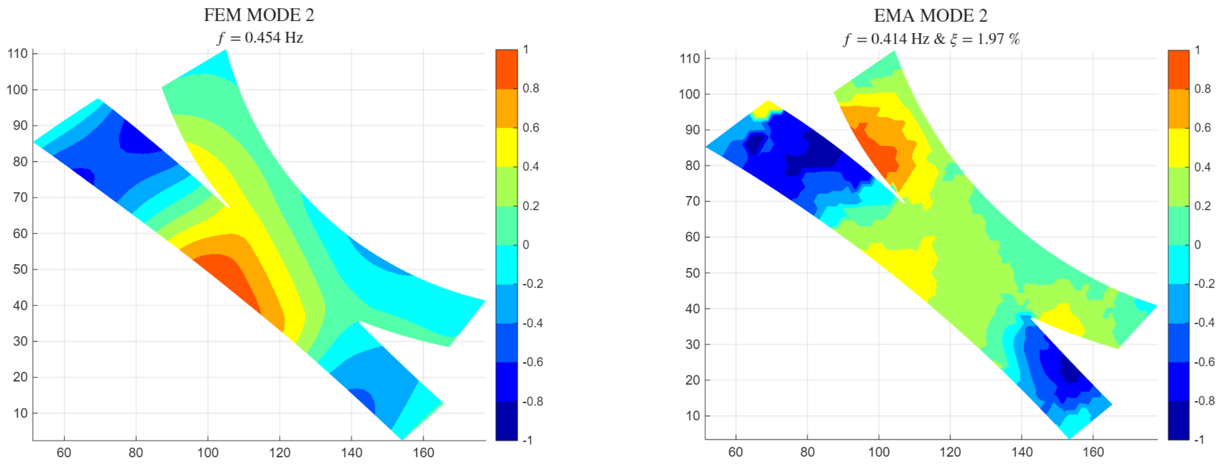

Figure 1.24: Comparison between FEM and EMA of mode 2

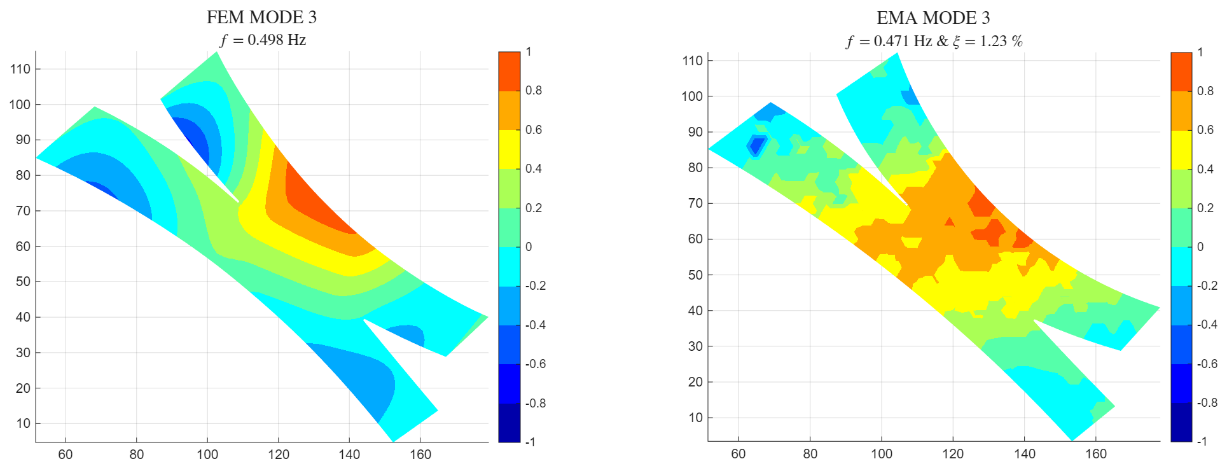

Figure 1.25: Comparison between FEM and EMA of mode 3

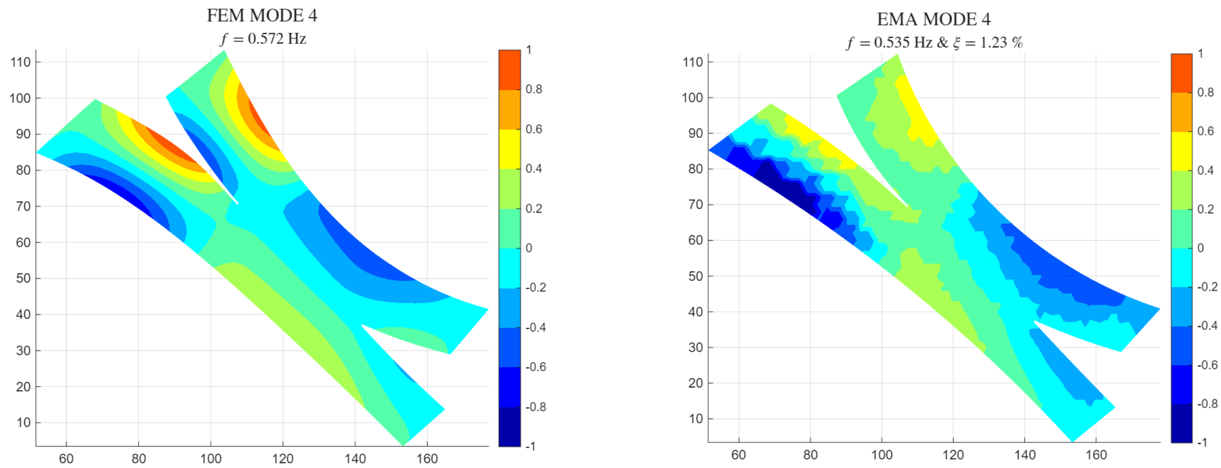

Figure 1.26: Comparison between FEM and EMA of mode 4

1.4 Comparison between EMA and FEM

Now that we represented both FEM and EMA plots, we conclude our analysis by comparing the two models with a statistical tool, that is the *MAC*.

The Modal Assurance Criterion (MAC) is a statistical indicator used to establish the degree of correlation between two sets of mode shapes, typically comparing experimental results with numerical predictions from Finite Element Models (FEM). It provides a scalar value ranging from 0 to 1, where a value of 1 represents a perfect correlation (the two modes coincide) and 0 indicates no correlation. This criterion, in this case, is used for comparing the FEM and EMA model.

The MAC can be defined as:

$$MAC(A,X) = \frac{\left|\sum_{j=1}^{n} \Phi_{X,j} \cdot \Phi^*_{A,j}\right|^2}{\left(\sum_{j=1}^{n} \Phi_{X,j} \cdot \Phi^*_{X,j}\right) \cdot \left(\sum_{j=1}^{n} \Phi_{A,j} \cdot \Phi^*_{A,j}\right)}, \tag{1.16}$$

where $\Phi_{X,j}$ and $\Phi_{A,j}$ are the mode shapes referred to FEM and EMA, respectively, while n is the number of sensors, i.e. measurement points composing the mesh.

MAC analysis gives us the following result:

Table 1.4: MAC values for each mode

Mode	MAC
1	0.9385
2	0.6221
3	0.5967
4	0.6694

The main drawback of MAC is that it isn't able to find in which degrees of freedom the modes are different. To solve such issue, a second index, called Coordinate Modal Assurance Criterion (CoMAC), can be used. It considers each DOF separately, summing on the modes:

$$CoMAC(j) = \frac{(\sum_{g=1}^{M} \left| \Phi_{X,j}^{(g)} \Phi_{A,j}^{(g)} \right|)^2}{(\sum_{g=1}^{M} \Phi_{X,j}^{(g)})^2 (\sum_{g=1}^{M} \Phi_{A,j}^{(g)})^2}, \tag{1.17}$$

where M is the number of modes considered and $\Phi_{X,j}^{(g)}$ and $\Phi_{A,j}^{(g)}$ are the j^{th} components of the eigenvectors associated to the g^{th} mode of the structure modeled with FEM and with EMA, respectively.

Since we would obtain CoMAC values for 202 sensors, the Figure 1.27 is helpful to visualize the results directly on the structure.

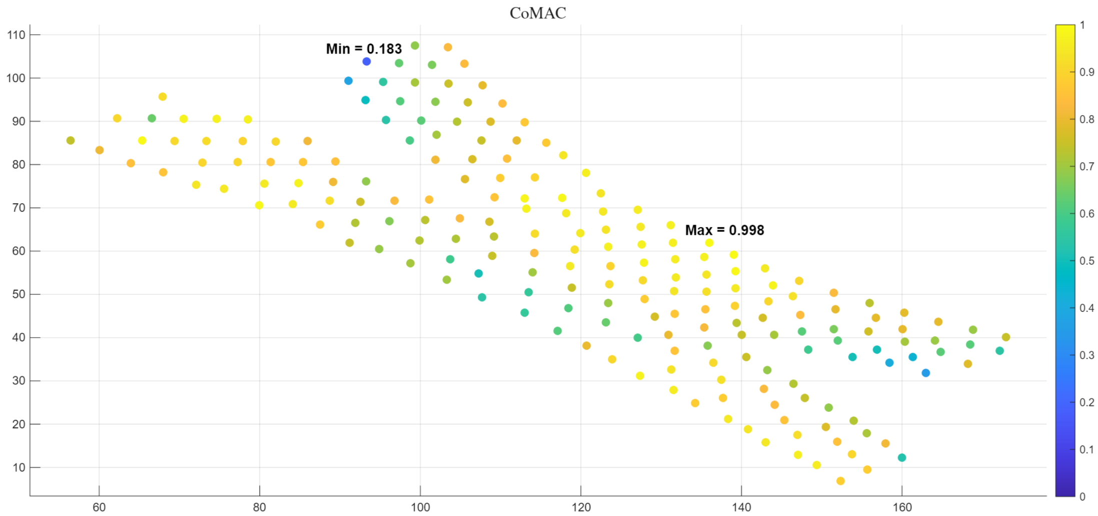

Figure 1.27: CoMAC displayed on the structure

Final remarks

As engineering students, we particularly appreciate to start applying our mathematical and physical background to solve real and complex engineering systems, and, as a result, this report is interested in highlighting how and, most importantly, why we obtained certain results. This work is the direct outcome of a group which invested on collaboration and commitment.